ISSN 1674-1056
http://cpb.iphy.ac.cn
http://iopscience.iop.org/cpb
中国物理 B
Chinese Physics
中国物理 Chinese Physics B

Temperature-dependent Raman spectroscopic study of ferroelastic $K_2Sr(MoO_4)$

Ji Zhang(张季), De-ming Zhang(张德明), Ran-ran Zhang(张冉冉)
Citation: Chin. Phys. B . 2018, 27(11): 117801. **doi:** 10.1088/1674-1056/27/117801
Journal homepage: http://cpb.iphy.ac.cn; http://iopscience.iop.org/cpb

What follows is a list of articles you may be interested in

Different angle-resolved polarization configurations of Raman spectroscopy: A case on the basal and edge plane of two-dimensional materials

Xue-Lu Liu(刘雪璐), Xin Zhang(张昕), Miao-Ling Lin(林妙玲), Ping-Heng Tan(谭平恒)
Chin. Phys. B . 2017, 26(6): 067802. **doi:** 10.1088/1674-1056/26/6/067802

High-temperature Raman spectroscopic study of vanadoborate $Na_3VO_2B_6O_{11}$

Ji Zhang(张季), De-Ming Zhang(张德明), Qing-Li Zhang(张庆礼), Shao-Tang Yin(殷绍唐)
Chin. Phys. B . 2016, 25(3): 037802. **doi:** 10.1088/1674-1056/25/3/037802

Doping inhomogeneity and staging of ultra-thin graphite intercalation compound flakes probed by visible and near-infrared Raman spectroscopy

Lu Yan, Zhang Xin, Wu Jiang-Bin, Li Xiao-Li, Li Qiao-Qiao, Tan Ping-Heng
Chin. Phys. B . 2015, 24(7): 077804. **doi:** 10.1088/1674-1056/24/7/077804

Temperature-dependent Raman spectroscopic study of bismuth borate $Bi_2ZnOB_2O_6$

Zhang Ji, Zhang De-Ming, Zhang Qing-Li, Yin Shao-Tang
Chin. Phys. B . 2015, 24(1): 017801. **doi:** 10.1088/1674-1056/24/1/017801

Three-dimensional noble-metal nanostructure：A new kind of substrate for sensitive, uniform, and reproducible surface-enhanced Raman scattering

Tian Cui-Feng, You Hong-Jun, Fang Ji-Xiang
Chin. Phys. B . 2014, 23(8): 087801. **doi:** 10.1088/1674-1056/23/8/087801

Temperature-dependent Raman spectroscopic study of ferroelastic $K_2Sr(MoO_4)$*

Ji Zhang(张季)[1,†], De-Ming Zhang(张德明)[2], and Ran-Ran Zhang(张冉冉)[3]

[1] An Hui Xin Hua University, Hefei 230088, China
[2] Anhui Institute of Optics and Fine Mechanics, Chinese Academy of Sciences, Hefei 230031, China
[3] High Magnetic Field Laboratory of the Chinese Academy of Sciences, Hefei 230031, China

(Received 2 July 2018; revised manuscript received 9 August 2018; published online 19 October 2018)

Raman scattering measurements of $K_2Sr(MoO_4)_2$ were performed in the temperature range of 25–750 °C. The Raman spectrum of the low-temperature phase α-$K_2Sr(MoO_4)_2$ that was obtained by first-principle calculations indicated that the Raman bands in the wavenumber region of 250–500 cm^{-1} are related to Mo–O bending vibrations in MoO_4 tetrahedra, while the Raman bands in the wavenumber region of 650–950 cm^{-1} are attributed to stretching vibrations of Mo–O bonds. The temperature-dependent Raman spectra reveal that $K_2Sr(MoO_4)_2$ exhibits two sets of modifications in the Raman spectra at $\sim$ 150 °C and $\sim$ 475 °C, attributed to structural phase transitions. The large change of the Raman spectra in the temperature range of 150 °C to 475 °C suggests structural instability of the medium-temperature phase β-$K_2Sr(MoO_4)_2$.

Keywords: ferroelastics, $K_2Sr(MoO_4)_2$ crystal, Raman spectroscopy, phase transition

PACS: 78.30.–j, 81.70.–q, 63.70.+h **DOI:** 10.1088/1674-1056/27/11/117801

1. Introduction

In recent years, various active dielectric materials and ferroelectrics have been extensively investigated in terms of their synthesis methods, crystal structures, and phase transitions owing to their applications in acoustoelectric devices, logic and memory elements, optic shutters, and so on. These applications are based on adjustment of crystal orientations and control of their domain structures by small mechanical and thermal deformations.[1] A large promising family of ferroelastics with general formulas of $M_3(XO_4)_2$ (M = Sr, Ba, Pb; X = P, As, V, Cr), $A_2M(XO_4)_2$ (A = K, Rb, Cs, Tl; M = Sr, Ba, Pb; X = S, Se, Cr, Mo, W), and $A_5R(Mo_4)_4$ (A = K, Rb, Tl; R = RE, Y, Bi, Fe) is characterized by tetrahedral XO_4 anions in their structures.[2–6] Among the ferroelastics, double molybdate $K_2Sr(MoO_4)_2$ containing MoO_4 tetrahedra is a new ferroelastic compound with the same palmierite-like structure as that of $Pb_3(MoO_4)_2$ and $B_2Pb(MoO_4)_2$ (B = K, Rb, Cs).[7] According to the study of Galiba,[8] $K_2Sr(MoO_4)_2$ crystallizes in a monoclinic phase (referred to as α-phase with a space group of $C2/c$) at a low temperature, which is similar to that of $Pb_3(MoO_4)_2$. At a high temperature of approximately 744 K, $K_2Sr(MoO_4)_2$ transitions to the $K_2Pb(SO_4)_2$-type phase (referred to as γ-phase with a space group of $R\bar{3}m$). In addition to the low- and high-temperature phases, a medium-temperature phase has been demonstrated by x-ray diffraction (XRD) of $K_2Sr(MoO_4)_2$ at 573 K. However, the crystal structure change is continuous and complex. To understand the crystallographic changes with temperature, further studies on the transformation of the crystal structure upon temperature variations are required.

Because Raman spectroscopy is an efficient method to investigate crystal structures, temperature-dependent Raman spectroscopy is frequently used to study phase transitions.[9–11] In this study, the Raman spectrum of $K_2Sr(MoO_4)_2$ was calculated by density functional theory (DFT) to help us assign the vibration modes. Temperature-dependent Raman spectra were then measured to study the structural changes of the $K_2Sr(MoO_4)_2$ system at different temperatures.

2. Experimental and computational methods

$K_2Sr(MoO_4)_2$ polycrystalline powder was prepared by conventional solid-state reactions. K_2CO_3, $SrCO_3$, and MoO_3 (analytic grade) were homogeneously mixed with appropriate proportions in an agate mortar and packed into a Pt crucible. The sample was heated slowly to 580 °C and maintained at this temperature for 80 h with several intermediate grindings and mixings. Powder-XRD measurements were performed in the range of 10°–70° with a step of 0.02°.

Room- and high-temperature Raman spectroscopy measurements were performed in the range of 100–1100 cm^{-1}. The sample was heated in a home-made heating furnace. The temperature was monitored by a thermocouple attached to the metal sample holder and controlled by a temperature controller within 1 °C. Raman spectra were acquired with a Horiba Jobin Yvon Raman spectrometer (LabRam800HR) in a backscatter-

*Project supported by the Natural Science Foundation of Anhui Province, China (Grant Nos. KJ2018A0588 and KJ2017A625).
†Corresponding author. E-mail: 18956063545@189.cn
© 2018 Chinese Physical Society and IOP Publishing Ltd

ing configuration. An ultraviolet light pulse with a wavelength of 355 nm and repetition frequency of 10 kHz from a coherent Innova ultra-laser was focused onto the sample using a Raman microprobe with a 4× objective lens. An intensified charge coupled device (CCD) was used to collect the scattering light. The sample was steadily heated from room temperature to 750 °C in a platinum boat placed in the center of the chamber. Each spectral acquisition (accumulation mode) was performed for 10 s, the average power of the laser operation was fixed to 800 mW, and the slit width was set to 300 nm for all measurements under different temperatures.

Structure optimization and calculations of the band structure, density of states, and Raman spectrum were performed using the CASTEP code[12] based on density functional theory (DFT). Conserving pseudopotentials were employed; the exchange–correlation was modeled using the Perdew–Burke–Ernzerhof (PBE)[13] functional, based on generalized gradient approximation (GGA).[14,15] The cut-off energy for the plane-wave basis set and k-point separation were chosen based on the criterion of fine precision. The structure optimization was performed until the forces on the atoms were smaller than 0.01 eV/Å, the energy change per atom smaller than 10^{-5} eV, and the stress components smaller than 0.05 GPa. Pseudo-atomic calculations were performed for O $2s^2 2p^4$, K $3s^2 3p^6 4s^1$, Sr $4s^2 4p^6 5s^2$, and Mo $4d^5 5s^1$. The other parameters used in the calculations had the default values of the CASTEP code.[16]

3. Results and discussion

3.1. Structures and factor group analyses

The XRD pattern of the sample is shown in Fig. 1. Comparison with the results of Galiba[8] shows that the obtained structure is α-$K_2Sr(MoO_4)_2$. The α-$K_2Sr(MoO_4)_2$ structure has a space group of $C2/c$ with lattice parameters of $a = 14.318$ Å, $b = 5.933$ Å, $c = 10.422$ Å, and $\beta = 105.83$ °C. The structure of α-$K_2Sr(MoO_4)_2$ is shown in Fig. 1. The K and Sr atoms are located at the M_1 and M_2 positions with distances of M_1–O in the range of 2.578–2.789 Å and M_2–O in the range of 2.605–3.161 Å. In addition, MoO_4 tetrahedra with Mo–O bond lengths of 1.747–1.767 Å[8] share vertices and edges with M_1 and M_2 polyhedra. These polyhedra alternatively arrange to form a layered structure parallel to the (100) plane.

The α-$K_2Sr(MoO_4)_2$ crystal is monoclinic, with a space group of $C2/c$ and two molecular formulae per unit cell ($Z = 2$). A group theoretical analysis of the normal modes of vibration of the α-$K_2Sr(MoO_4)_2$ structure at $q = 0$ predicts the following decomposition for the two formula units of the crystal in the primitive cell, according to the irreducible representations of the point group C_{2h}.[17] Excluding acoustic modes A_u+2B_u, the Raman spectrum should contain $37A_u+40B_g$ normal modes of vibration.

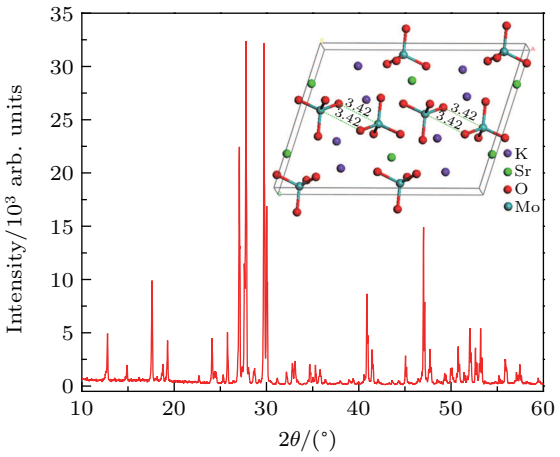


Fig. 1. (color online) Powder-XRD pattern and structure (inset) of the α-$K_2Sr(MoO_4)_2$ crystal.

3.2. Raman spectrum at room temperature

The measured Raman spectrum of α-$K_2Sr(MoO_4)_2$ at room temperature in the range of 100–1100 cm^{-1} is presented with the black line in Fig. 2, while the calculated (with the first-principles method) Raman spectrum of α-$K_2Sr(MoO_4)_2$ is presented with the red line. The calculated spectrum fits well with the experimental one. In the Raman spectrum, the bands can be grouped into three regions. The wavenumber region of 100–250 cm^{-1} consists of four bands at 110 cm^{-1}, 138 cm^{-1}, 180 cm^{-1}, and 235 cm^{-1}, which are fundamental transitions for translational and rotational lattice vibrations. The low-frequency bands in this region are assigned to external modes, related to translations of Sr^{2+}, K^+, and MoO_4 clusters. The assignments of the external modes are based on the previous studies about Raman spectra of acousto-optic $NaBi(MoO_4)_2$, ferroelastic orthorhombic $Gd_2(MoO_4)_3$, and multilayer $KY(MoO_4)_2$ crystal with Raman active external modes below 200 cm^{-1}, 300 cm^{-1}, and 270 cm^{-1}, respectively.[18–20] To provide insights into the vibrations, Figure 3 illustrates representative vibration modes calculated by DFT. Figure 3(c) illustrates the lattice vibration for the Raman band at 124 cm^{-1}, where Sr^{2+} and K^+ ions exhibit strong vibrations.

The Raman bands around 250–500 cm^{-1} and 650–950 cm^{-1} are assigned to internal modes corresponding to the Mo–O vibrations of MoO_4 tetrahedra. It is well known that a MoO_4 tetrahedron molecule with a T_d symmetry has four normal vibrational modes: ν_1 (symmetric stretching mode), ν_2 (bending mode), ν_3 (asymmetric stretching mode), and ν_4 (bending mode).[21,22] It is commonly observed that the stretching modes have higher vibration frequencies than the bending modes. For example, Mo–O bending vibrations were observed in the frequency regions of 320–404 cm^{-1} and 277–465 cm^{-1} in the spectra of $NaBi(MoO_4)_3$ and $KY(MoO_4)_2$

crystals, respectively, while the Raman bands of stretching vibration modes were observed at above 700 cm^{-1}. Therefore, in the Raman spectrum of α-$K_2Sr(MoO_4)_2$, the Raman bands at 315 cm^{-1}, 363 cm^{-1}, and 384 cm^{-1} are related to Mo–O bending vibrations, while the Raman bands at 711 cm^{-1}, 795/810 cm^{-1}, 844/858 cm^{-1}, 887 cm^{-1}, and 899/904 cm^{-1} are attributed to Mo–O stretching vibrations. Figures 3(a) and 3(b) illustrate representative vibration modes of the Raman bands at (a) 899 cm^{-1} (Mo–O stretching vibration) and (b) 320 cm^{-1} (Mo–O bending vibration). Therefore, the calculated results are valuable in the assignment of the vibration modes. The assignments of the observed vibrational wavenumbers at room temperature are presented in Table 1.

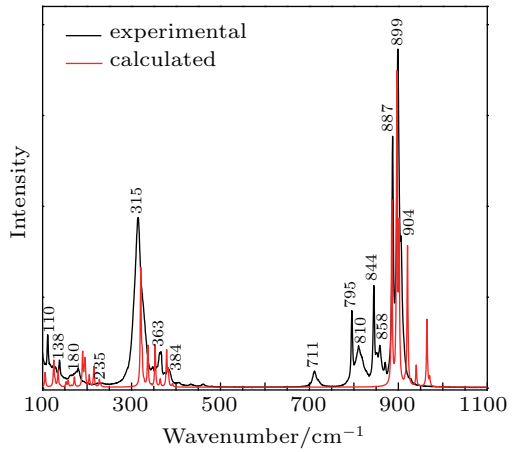


Fig. 2. (color online) Experimental and calculated Raman spectra of the $K_2Sr(MoO_4)_2$ crystal at room temperature.

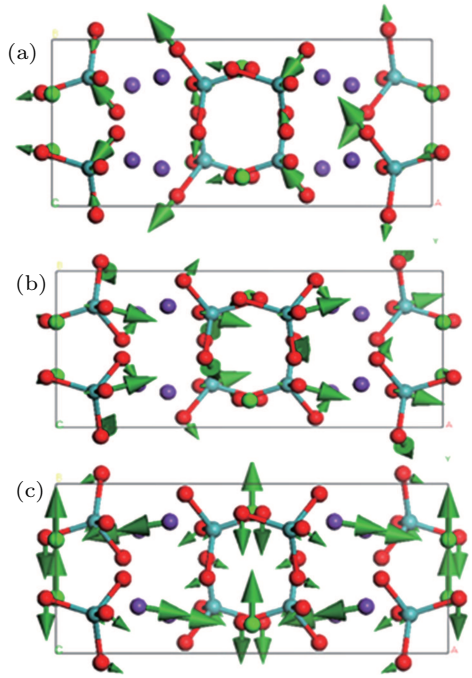


Fig. 3. (color online) Illustration of representative vibration modes: (a) Raman band at 899 cm^{-1} with Mo–O stretching vibration, (b) Raman band at 320 cm^{-1} with Mo–O bending vibration, and (c) Raman band at 124 cm^{-1} with lattice vibration.

Table 1. Raman shifts and assignments for the α-$K_2Sr(MoO_4)_2$ crystal at room temperature.

Raman shift /cm^{-1}		Assignment
Experimental	Calculated	
110	116	lattice vibration
138	137	
180	174	
235	–	
315	314	Mo–O bending vibration in $[MoO_4]$
363	352	
384	–	
711	–	Mo–O stretching vibration in $[MoO_4]$
795/810	–	
844/858	845	
887	869	Mo–O stretching vibration in $[MoO_4]$
899	898	

It is worth noting that a considerable splitting of the vibration levels corresponding to the Mo–O stretching vibration is observed. The frequency difference between the v_1 and v_3 modes is as large as 200 cm^{-1} in the Raman spectrum of α-$K_2Sr(MoO_4)_2$. These frequency differences are also observed in the Raman spectra of $KY(MoO_4)_2$ (280 cm^{-1}) and $NaBi(MoO_4)_2$ (230 cm^{-1}); however, the difference for the tetrahedral molybdate ions does not exceed 150 cm^{-1}.[23–26] The stretching frequency region exhibits a large broadening owing to additional interactions between MoO_4^{2-} ions through relatively short (3.42 Å) bridge bonds in the unit cell, as shown in Fig. 1.

3.3. High-temperature Raman spectra

The $K_2Sr(MoO_4)_2$ crystal melts incongruently at 900 °C and has two distinct phase transitions at temperatures of $T_1 = 148$ °C and $T_2 = 471$ °C corresponding to polymorphic first-order transitions α (low-temperature)$\rightarrow$ β (medium-temperature)$\rightarrow$ γ (high-temperature). To better understand the structure changes of $K_2Sr(MoO_4)_2$, temperature-dependent Raman spectra of the $K_2Sr(MoO_4)_2$ crystal were recorded from room temperature to 750 °C, as presented in Fig. 4.

To provide further insights into the Raman bands' behaviors with the increase of the temperature, we analyzed the Raman wavenumber variations with the temperature (ω as a function of T).[27] The equation $\omega = \omega_0 + \alpha T$ (α is the linear coefficient of the curve) was obtained in the first approximation as the dependences of ω on T. The curves for each mode are plotted in Figs. 5 and 6. The wavenumbers of the bands of 111 cm^{-1}, 138 cm^{-1}, and 180 cm^{-1} shift almost linearly toward higher values (Fig. 6), as these bands are attributed to the external vibrations related to motions of K and Sr atoms. However, the high-wavenumber bands at 711 cm^{-1}, 795 cm^{-1}, 810 cm^{-1}, and 899 cm^{-1} become softened with smaller slope coefficients at the first transition point (approximately 150 °C).

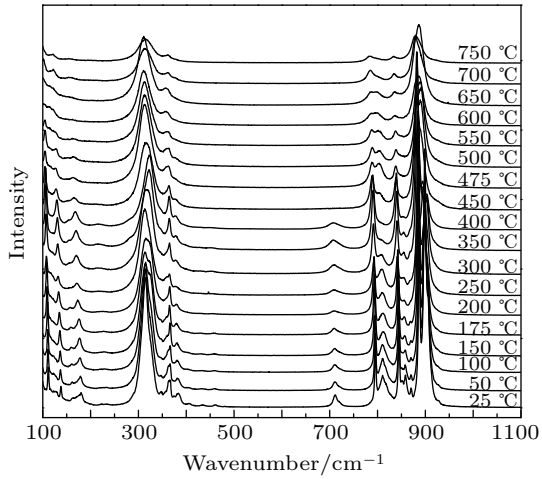


Fig. 4. Temperature-dependent Raman spectra of $K_2Sr(MoO_4)_2$ in the range of 25–750 °C.

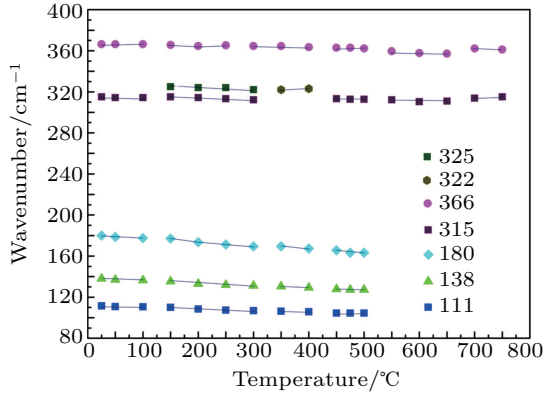


Fig. 5. (color online) Wavenumber shifts of Raman bands in the spectral range of 100–350 cm^{-1} with the increase of the temperature.

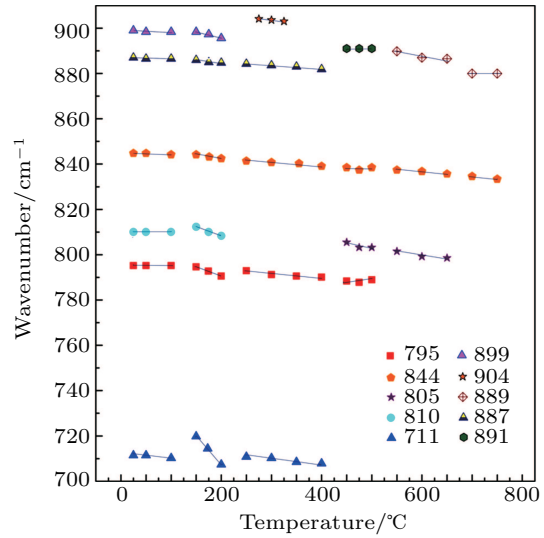


Fig. 6. (color online) Wavenumber shifts of Raman bands in the spectral range of 700–950 cm^{-1} with the increase of the temperature.

Compared to the wavenumber shifts, the appearance of new bands better reflects the structure changes of $K_2Sr(MoO_4)_2$. Local enlarged views of the Raman spectra are shown in Figs. 7 and 8. In order to clearly show the changes of the Raman bands, different line styles were used at different temperature ranges. In the low-wavenumber region of 300 cm^{-1} to 340 cm^{-1}, the intensity of the shoulder band at 324 cm^{-1} began to increase at 150 °C, corresponding to the first phase transition. This shoulder band continued to increase and merged into a broadened band with a main band at 314 cm^{-1}. However, with the increase in the temperature, the band at 314 cm^{-1} disappeared and only one band remained at 350 °C, represented by the blue dotted lines. After the temperature reached the second phase-transition point of 475 °C, the Raman spectra became stable. Band changes are also observed at the high-wavenumber region. The Raman band at 894 cm^{-1} in the plot at 300 °C disappeared when the temperature increased to 350 °C. A band at 890 cm^{-1} was generated and merged with the band at 880 cm^{-1} into a broadened band when the sample was heated to 450 °C. In particular, a larger change was observed between 350 °C and 475 °C. These changes of the spectra suggest that the crystal structure of the medium-temperature phase is not stable in the temperature range of

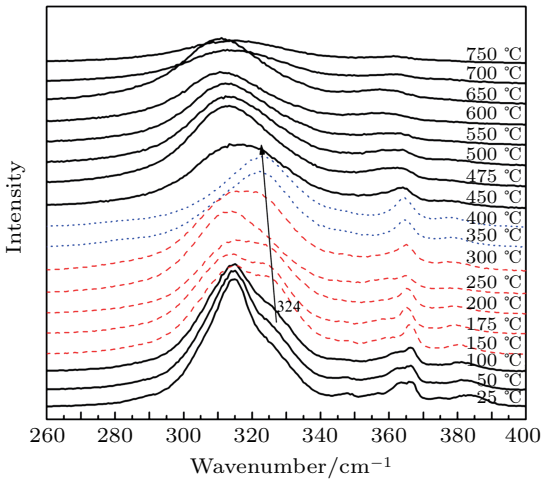


Fig. 7. (color online) Local enlarged image of the temperature-dependent Raman spectra in the range of 260–400 cm^{-1}.

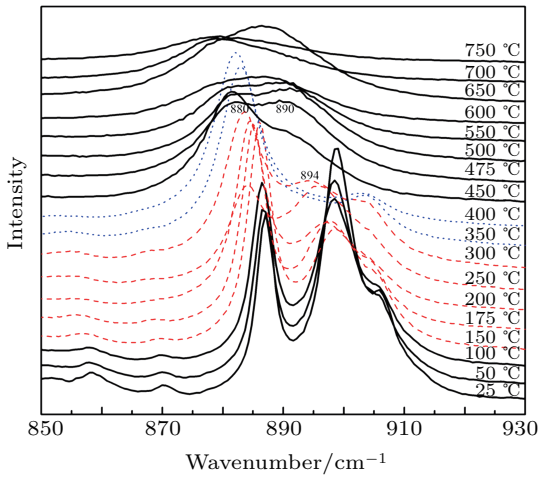


Fig. 8. (color online) Local enlarged image of the temperature-dependent Raman spectra in the range of 850–930 cm^{-1}.

150 °C to 475 °C. It is worth noting that the Raman intensities of the low-wavenumber bands at 110 cm^{-1}, 138 cm^{-1}, and 180 cm^{-1} (related to the vibrations of K^+ and Sr^{2+} cations) significantly decreased when the temperature increased above 475 °C. These bands were almost not observed at 600 °C. According to a study on a palmierite-related $K_5Yb(MoO_4)_4$ crystal,[28] the occupations of M_1 and M_2 positions change from ordered type to statistical with the increase of the temperature. The disappearance of these low-wavenumber bands suggested further disordering of K^+ and Sr^{2+} cations at high temperatures.

4. Conclusion

We performed a detailed investigation on the Raman spectrum of α-$K_2Sr(MoO_4)_2$ using first-principle calculations. The structural changes were discussed based on the temperature-dependent Raman spectra. The calculated Raman spectrum of α-$K_2Sr(MoO_4)_2$ was in good agreement with the experimental result. The Raman bands were mainly related to Mo–O vibrations in MoO_4 tetrahedra. The temperature-dependent Raman spectra revealed that $K_2Sr(MoO_4)_2$ exhibited two sets of modifications in the Raman spectra, at $\sim$ 150 °C and $\sim$ 475 °C. These modifications were attributed to structural phase transitions. The large change of the Raman bands in the temperature range of 150 °C to 475 °C showed that the structure of the medium-temperature phase β-$K_2Sr(MoO_4)_2$ was not stable.

Acknowledgment

The authors thank the High-Magnetic-Field Laboratory of the Chinese Academy of Sciences for the use of their Raman spectrometer.

References

[1] Janovec V and Přívratska J 2006 *Int. Tables Crystallogr. Dch.* **3** 4
[2] Efremov V A and Trunov V K 1974 *Crystallogr. Rep.* **19** 989
[3] Trunov V K, Efremov V A and Velikodny Yu A 1986 *Crystal Chemistry and Properties of Double Molybdates and Tungstates* (Leningrad: Nauka)
[4] Dudnik E F and Kiosse G A 1983 *Bull. Acad. Sci. USSR Phys. Ser.* **47** 420
[5] KepplerU 1970 *Z. Kristallogr.* **132** 228
[6] Guimaraes D M C 1979 *Acta Crystallogr. A* **35** 108
[7] Trunov V K 1971 *Russ. J. Inorg. Chem.* **16** 553
[8] Tsyrenova G D, Pavlova E T, Solodovnikov S F, Popova N N, Kardash T Y, Stefanovich S Y, Gudkova I A, Solodovnikova Z A and Lazoryak B I 2016 *J. Solid State Chem.* **237** 64
[9] Zhang J, Zhang D, Zhang Q and Yin S 2016 *Chin. Phys. B* **25** 037802
[10] Cerderira F, Melo F E A and Lemos V 1983 *Phys. Rev. B* **27** 7716
[11] Zhang J, Zhang D, Zhang Q and Yin S 2015 *Chin. Phys. B* **24** 017801
[12] Segall M D, Lindan P J D, Probert M J, Pickard C J, Hasnip P J, Clark S J and Payne M C J 2002 *J. Phys.: Condens. Matter* **14** 2717
[13] Perdew J P, Burke K and Ernzerhof M 1996 *Phys. Rev. Lett.* **77** 3865
[14] Perdew J P 1991 *Electron. Struct. Solids* **17** 11
[15] Perdew J P, Burke K and Wang Y 1996 *Phys. Rev. B* **54** 16533
[16] Goodwin A L, Calleja M, Conterio M J, Dove M T and Evans J S O 2005 *Z. Kristallogr.* **220** 567
[17] Zhang G Y 2001 *Lattice Vibrational Spectroscopy* (Beijing: Higher Education Press)
[18] Hanuza J and Labuda L 1981 *J. Raman Sprctrosc.* **11** 231
[19] Moiseenko V N, Bogatirjov Yu I, Jeryemenko A M and Akimov S V 2000 *J. Raman Sprctrosc.* **31** 539
[20] Kaminsk A A, Eichler H J, Grebe D, Macdonald R, Bagaev S N, Pavlyuk A A and Kuznetsov F A 1996 *Phys. Stat. Sol.* **153** 281
[21] Kamitsos E I, Karakassides M A and Chryssikos G D 1989 *Phys. Chem. Glasses* **30** 229
[22] Heyns A M, Range K J and Wildenauer M 1990 *Spectrochim. Acta A* **46** 1621
[23] Brown R G, Denning J, Hallett A and Ross S D 1970 *Spectrochim. Acta Part. A* **26** 963
[24] Khanna R K and Lippincott E R 1968 *Spectrochim. Acta Part. A* **24** 905
[25] Scott J F and Porto S 1967 *Phys. Rev.* **157** 716
[26] Nikol M and Durana F 1971 *J. Chem. Phys.* **54** 1436
[27] Silva K P D, Coelho J S, Maczka M, Paraguassu W and Freire P T C 2013 *J. Solid State Chem.* **199** 7
[28] Morozov V A, Lazoryak B I, Lebedev O I, Amelinckx S and Tendeloo V G 2003 *J. Solid State Chem.* **176** 76